A high-power subterahertz surface wave oscillator with separated overmoded slow wave structures*

Guang-Qiang Wang(王光强)[1,2], Jian-Guo Wang(王建国)[1,3,†], Peng Zeng(曾鹏)[1,2], Dong-Yang Wang(王东阳)[1,2], and Shuang Li(李爽)[1,2,3]

[1] *Northwest Institute of Nuclear Technology, Xi'an* 710024, *China*
[2] *Science and Technology on High Power Microwave Laboratory, Xi'an* 710024, *China*
[3] *School of Electronic and Information Engineering, Xi'an Jiaotong University, Xi'an* 710049, *China*

(Received 26 May 2016; revised manuscript received 22 August 2016; published online 25 October 2016)

A megawatt-level subterahertz surface wave oscillator (SWO) is proposed to obtain high conversion efficiency by using separated overmoded slow wave structures (SWSs). Aiming at the repetitive operation and practical applications, the device driven by electron beam with modest energy and current is theoretically analyzed and verified. Then, the functions of the two SWS sections and the effect of the drift tube are investigated by using a particle-in-cell code to reveal how the proposed device achieves high efficiency. The mode analysis of the beam-wave interaction region in the device is also carried out, and the results indicate that multi-modes participate in the premodulation of the electron beam in the first SWS section, while the TM_{01} mode surface wave is successfully and dominantly excited and amplified in the second SWS section. Finally, a typical simulation result demonstrates that at a beam energy of 313 keV, beam current of 1.13 kA, and guiding magnetic field of above 3.5 T, a high-power subterahertz wave is obtained with an output power of about 70 MW at frequency 146.3 GHz, corresponding to the conversion efficiency of 20%. Compared with the results of the previous subterahertz overmoded SWOs with integral SWS and similar beam parameters, the efficiency increases almost 50% in the proposed device.

Keywords: terahertz, surface wave oscillator, mode selection, particle simulation

PACS: 84.40.Fe, 45.10.Db, 52.65.–y **DOI:** 10.1088/1674-1056/25/12/128401

1. Introduction

Devices generating narrow-band high-power pulses at frequencies ranging from microwave to terahertz wave band are of great significance due to their military applications in radar, direct energy weapon, and electromagnetic jam.[1–3] Detecting concealed radioactive materials is also one of the promising applications.[4] For the merits of high efficiency and simple structure, several kinds of vacuum electronic devices have attracted more attention,[5–14] such as relativistic backward wave oscillator (BWO), multiwave Cerenkov generator (MWCG), and surface wave oscillator (SWO). As one of the promising candidates at high frequencies, the SWO with overmoded structure utilizes an intense electron beam interacting with a surface wave excited in the slow wave structure (SWS) to obtain high-efficiency output and mitigate the fabrication difficulty. Up to now, a radiation power of 2.6 MW from an overmoded SWO with integral SWS in a 0.14-THz frequency band has been demonstrated experimentally.[15] However, the conversion efficiency of the design is less than expected. Though many efforts have been made by using coaxial structure or tapered SWS, the efficiencies extracted from simulation results are still no more than 14%.[16,17] In Ref. [18], a 0.14-THz overmoded SWO was designed with higher beam voltage and current to achieve a conversion efficiency of about 20%, and a single pulse power of 5 MW was obtained in the later experiment.[19] But the beam current is triple that of the previous repetitive device and so it is inappropriate for repetitive operation,[2,20] while the required high diode voltage obstructs the structure scaling-down and stability of the accelerator. Therefore, increasing the efficiency of overmoded SWO aiming at the repetitive operation is still urgent at high frequencies such as subterahertz frequency band.

Based on the separated overmoded SWSs, a high-power subterahertz SWO with high efficiency is proposed and analyzed in this paper. In Section 2, a brief description of our design is introduced, and the feasibility of fundamental mode operation for electron beam with moderate energy and current is preliminarily discussed. In Section 3, the working process of the device is investigated with the particle-in-cell (PIC) simulations to elucidate why it has a high-efficiency output, and the influences of some key parameters are presented. Finally, a summary is presented in Section 4.

2. Description of the device model

As mentioned above, some structure improvements of the subterahertz SWO based on an integral SWS have not deliv-

*Project supported by the National Natural Science Foundation of China (Grant No. 61231003).
†Corresponding author. E-mail: wanguiuc@mail.xjtu.edu.cn
© 2016 Chinese Physical Society and IOP Publishing Ltd

ered the anticipated increase of efficiency. On the other hand, among various overmoded slow-wave devices, the MWCG has obtained a record output of about 15 GW at X band due to the use of the dual-section SWSs,[10] which is thought to be of advantage for the beam-wave energy conversion because the region of modulation is separated from the region of energy extraction. Moreover, a similar structure has been successfully employed in Ka band to achieve a conversion efficiency of about 35% in simulation.[21] Therefore, we try to introduce the separated SWSs into the subterahertz overmoded SWO to increase the efficiency. However, these devices are designed aiming at GW-class output, using an intense relativistic electron beam above 0.6 MeV and 5 kA,[10,21] that is, huge pulsed power supplies are required. But for repetitive operation and compactness at higher frequencies, the devices driven by electron beams with modest energy and current are preferable. So there are still some issues that need investigating in our following design.

Based on the previous work of subterahertz overmoded SWOs,[15,22,23] a 0.14-THz high-power SWO with separated overmoded SWSs is proposed, whose structure with parameters denoted is schematically shown in Fig. 1 (because of its axial symmetry, only half of the axial section is presented here). The first and second SWS sections are denoted as SWS1 and SWS2, respectively. Sharing many similarities with the conventional MWCG, the unique features of this device are as follows: (i) the radiation frequency is as high as 140 GHz, so high period number of SWS is required and the structural parameters become much smaller; (ii) it is driven by a modest energy electron beam below 400 keV; (iii) a relatively low beam current of less than 1.5 kA is used.

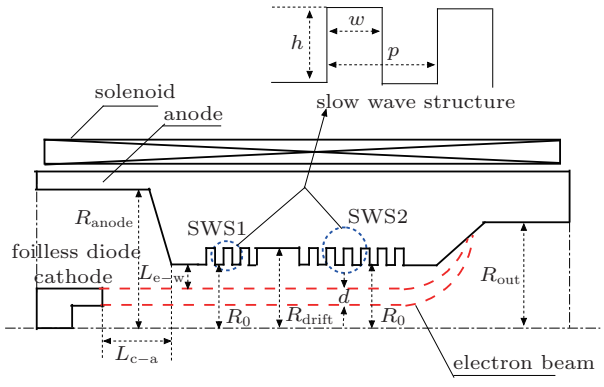


Fig. 1. (color online) Schematic diagram of the proposed SWO.

Table 1 summarizes the selected main dimensions of the structure in our device. The rectangularly corrugated SWSs are employed in both sections as usual for easy fabrication and high coupling impedance. Dispersion curves for the first three symmetric TM_{0n} modes of the overmoded SWS are calculated and shown in Fig. 2. The Doppler line of electron beam with an energy of 400 keV is depicted as an example, and it interacts with the TM_{01} mode at about 0.8π in the first Brillouin zone, which is so-called surface wave region as this part of the dispersion curve is below the light line. Moreover, the interaction point would be closer to π if the beam energy is lower. Thus the surface wave could interact with the electron beam having modest energy or lower, and the selected working point is of benefit to keeping the persistent beam-wave interaction as the beam loses energy. These have been validated in the former SWOs with integral SWSs.[15] However, in the proposed design here, the second SWS section (SWS2), where the intense beam-wave interaction occurs to yield high-power pulse, has smaller period number than the former. According to Ref. [24], there is a starting energy for oversized devices, which satisfies

$$\mathrm{Re}(|k_z - k_\mathrm{b}|) = \mathrm{Re}(\Delta k) = 2\pi|N|/L, \tag{1}$$

where k_z and k_b are respectively the wave number of excited structural wave and the beam mode, L is the length of SWS, and N is an integer corresponding to the spatial harmonic. Since the interaction point is at the fundamental harmonic zone, the starting energy is obviously independent of the length of SWS as $N = 0$ in Eq. (1). So the beam energy is in principle enough to drive the SWO with separated SWSs here. If lower beam energy is used that the electron beam interacts with -1st spatial harmonic, in fact, the SWS with 19 periods is still able to excite a subterahertz wave as indicated in Fig. 3.

Table 1. Structural parameters of the proposed 0.14-THz SWO.

Parameters	Values
Radius of anode, R_{anode}/mm	9
Thickness of electron beam, d/mm	0.5
Distance between electron beam and waveguide wall, L_{e-w}/mm	0.5
Distance between cathode and anode, L_{c-a}/mm	24
Radius of output waveguide, R_{out}/mm	4
Radius of drift tube, R_{drift}/mm	3.3
Inner radius of SWS, R_0/mm	3
Period length of SWS, p/mm	0.7
Depth of SWS, h/mm	0.3
Width of SWS, w/mm	0.4
Period number of SWS1 and SWS2	7/19

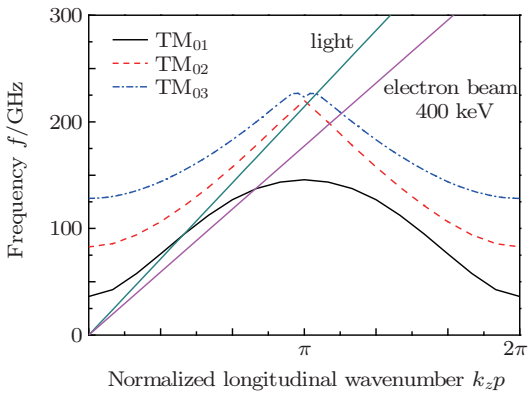


Fig. 2. (color online) Dispersion curves of TM_{01}, TM_{02}, and TM_{03} modes and the 400-keV beam Doppler line.

The interaction width Δk calculated based on the small-signal theory[22] roughly gives a starting energy of 50 keV, which is far below the expected beam energy. Accordingly, it is thought that it is feasible to drive the proposed device with a low energy electron beam.

Next, we examine the starting current of the proposed device. Due to the resonant reciprocal Bragg reflection of the counter-running and following waves in SWO,[5] the actual reflection coefficient within the overmoded SWS will be considerable. Based on the work by Levush *et al.* in Ref. [25], the starting currents are roughly estimated for three values of the combined reflection coefficient: $R = 0.3$, 0.5, and 0.7. As shown in Fig. 4, the reflection makes the device starting condition a sensitive function of beam energy, and the starting current is reduced accompanied with the enhancement of the reflection. But the starting currents at beam energy ranging from 100 keV to 400 keV are always no more than 300 A. Accordingly, the beam current of less than 1.5 kA is still adequate to excite the subterahertz wave in overmoded SWS with 19 periods.

The mode selection method of the TM_{01} mode in the proposed device is similar to the previous SWO. More details can be found in Refs. [15] and [18]. The specific results will be analyzed in the following PIC simulations.

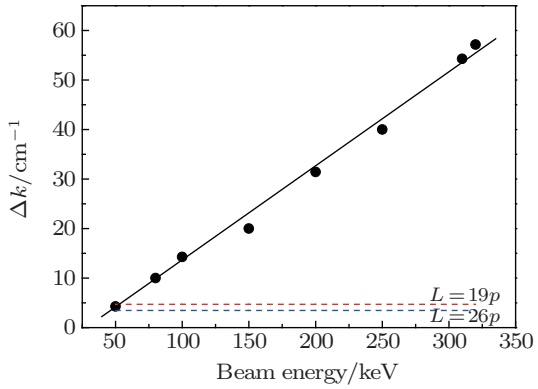


Fig. 3. (color online) Interaction width Δk versus beam energy at a beam current of 1 kA. The solid line represents the fitted curve of the discrete Δk (solid circles), and the dashed lines represent $2\pi/L$ for different values of L.

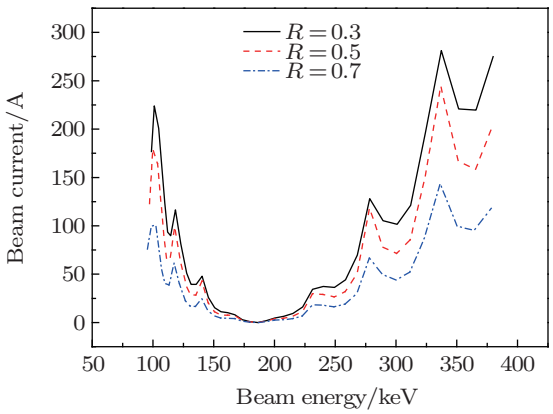


Fig. 4. (color online) Starting currents versus beam energy for different values of R.

3. PIC simulation

In order to figure out the working process of the SWO with separated SWSs, the PIC simulation investigations are carried out by using a PIC code UNIPIC,[26,27] which has been successfully used to design some high-frequency Cerenkov devices.[15–18] Besides, some results are compared with those from the device with integral SWS to interpret why the proposed SWO has a higher efficiency. In the following simulations, the beam energy is about 313 keV, the beam current is about 1.13 kA, and the guiding magnetic field is 5 T, unless specific parameters are clarified.

3.1. Function of each SWS section

The well-bunched electron beam in phase space at the moment of 10 ns is illustrated in Fig. 5. The steady-state result indicates that the intense electron beam is first modulated in the first SWS section (SWS1), and this beam modulation is greatly enhanced in SWS2, where the decelerated electrons lose their energies to achieve the excitation and amplification of subterahertz wave. This means that one important function of the first SWS section is to premodulate the electron beam, while the major beam-wave interaction indeed occurs in the second part. Thus, the presence of SWS1 will effectively reduce the required beam-wave interaction length, i.e., the periodic number of SWS2, to keep the device compact.

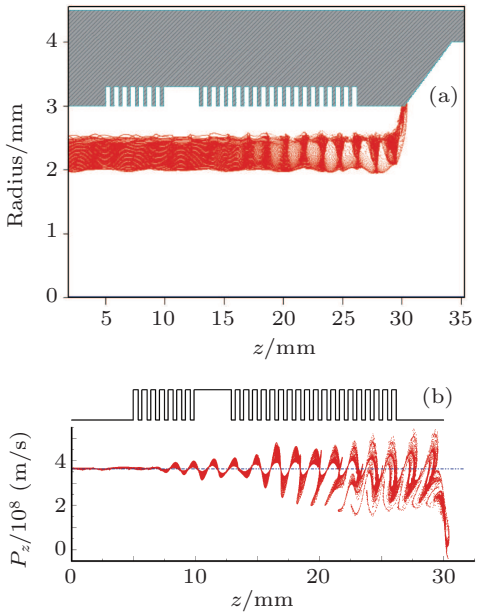


Fig. 5. (color online) Distributions of electrons and their momentum in (a) r–z space and (b) phase space.

Figure 6 shows the net power flow distribution along axial direction within the proposed SWO. The results for SWO with integral SWS under the same input and structural parameters are also depicted for comparison. First, there is an obvious reduction of the counter-running power flow in the diode region of the device with separated SWSs. That is to say, SWS1 acts a reflector to segregate the diode region from the beam-wave

interaction region. The power reflection coefficients of SWS1 for TM_{01}, TM_{02}, and TM_{03} modes, which are the non-cutoff TM_{0n} modes in the drift tube, are calculated and shown in Fig. 7. The oscillation frequency of 146.3 GHz stays out of the curve dips, and strong reflection of TM_{01} mode is found while the other two modes become weakened in turn. This reflection is of advantage to reduce the influence of the counter-running wave on the beam motion in the diode region and increase the output power according to the associated studies of Cerenkov oscillators.[1] In a sense, SWS1 is similar to a cascaded reflector employed in a recent overmoded device.[28]

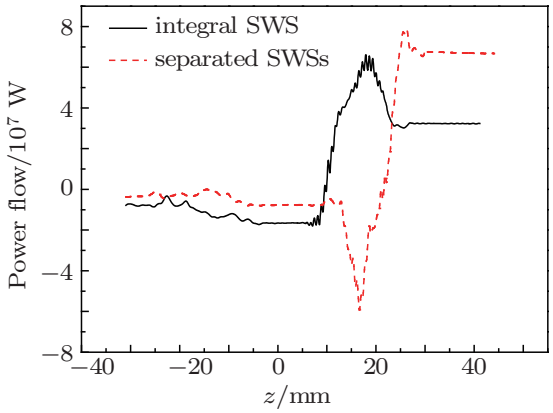


Fig. 6. (color online) Net power distributions in SWO.

Besides, there are two maximum values of power flows with opposite directions in SWS2. Unlike the scenario of the SWO with integral SWS, the peak value of counter-running power flow is just formed by the reflection of SWS1. The gap between the peak value of following power flow and output power becomes smaller. This can be explained as the decrease of the beam-wave interaction length, thereby resulting in the drop of the Q value and the corresponding increase of the energy leakage in SWS2. Moreover, this Q value happens to be optimal to a certain extent for the proposed device with current parameters. So more excited power gets out of the SWS, and thus a high-efficiency output is obtained.

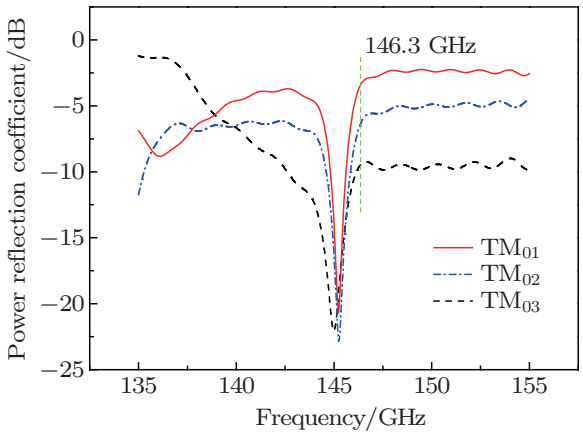


Fig. 7. (color online) Plots of power reflection coefficient versus frequency for different modes of SWS1.

3.2. Influence of the drift tube

As seen from Fig. 5(a), the bunching center of the electron beam becomes clearer and clearer from the drift tube to SWS2, implying the strong density modulation in SWS2, while figure 5(b) indicates that the velocity modulation of electron beam almost keeps constant in the drift tube region. Figure 8 shows the comparison between the axial momentum of electrons in integral SWS and separated SWSs. Due to the separation of the drift tube, the velocity modulation becomes very weak in SWS1, and it reaches the same extent as the one in integral SWS until in the back part of SWS2. Thus, the large velocity spread is avoided in the front section of SWS2, and more effective beam-wave interaction can be expected since more electrons keep synchronism with the surface wave. The axial beam power distributions in the two types of devices are also extracted from simulation results and shown in Fig. 9. The periodic power peaks are corresponding to the beam bunches presented in Figs. 5 and 8. Comparing the two curves in Fig. 9, it can be found that the maximal peak power in separated SWSs is much higher than the one in the integral SWS though the first few peaks are much smaller, and it roughly emerges in the center of SWS2. Then, the modulation amplitude of the beam power decreases greatly because it is transferred to the subterahertz wave field. Therefore, the drift tube is still a critical part in the proposed device as known in MWCGs at lower frequencies.

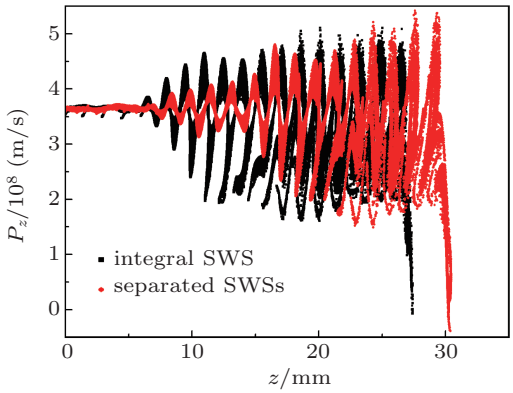


Fig. 8. (color online) Electron distributions in phase space for integrated SWS and separated SWSs.

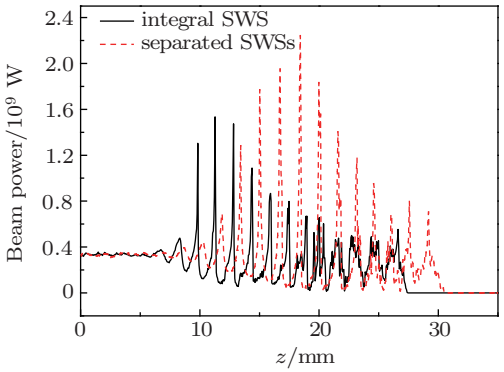


Fig. 9. (color online) Beam power distributions along axial direction for integrated SWS and separated SWSs.

The efficiency and frequency dependences on length and radius of the drift tube are investigated and shown in Fig. 10. It can be seen that the two parameters have great influences on the efficiency while the frequency is not so sensitive to them, especially the drift tube radius. The conversion efficiency roughly has a quasi-periodical dependence on drift tube length, and the period is about half the generated wavelength, i.e., 1 mm in our device. But the efficiency at a length of 3 mm is far above other peak values. When the drift tube radius varies, the output efficiency reaches its maximum value around 3.3 mm and monotonically decreases no matter the radius increases or decreases. So the performances of the SWO with separated SWSs at subterahertz frequency band are more sensitive to the structural parameters of the drift tube, and more attention should be paid to its manufacture and the later experiments.

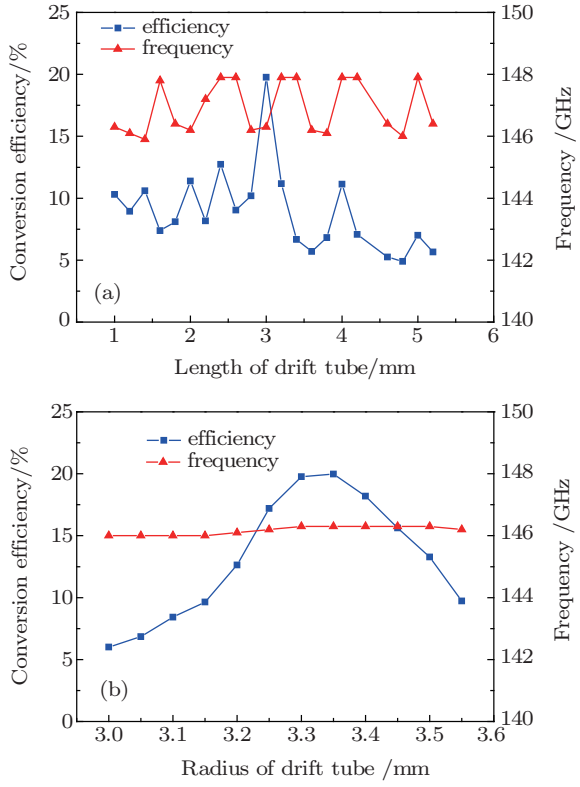


Fig. 10. (color online) Dependences of the efficiency and frequency on the length (a) and radius (b) of drift tube.

3.3. Mode analysis in overmoded SWSs

Based on the mode decomposition method proposed in Refs. [29] and [30], the compositions of TM_{0n} modes in the following (z) and counter-running ($-z$) directions in the drift tube are determined and given in Table 2. Obviously, multi-modes are generated, and the powers of TM_{02} and TM_{03} modes account for considerable proportions of the subterahertz wave in both directions. According to the reflection coefficents in Fig. 7, there must be certain power proportions of the two higher modes entering into SWS1. As the length of SWS1 is too short, its Q value is so small that the selection mechanism of TM_{01} mode by electron selection does not work.[5] That is, the higher modes originate from the inside conversion and outside import cannot be suppressed. Figure 11(a) gives the radial distribution of E_z in the middle of SWS1, and indicates the remarkable characteristic of volume wave since the E_z reaches its maximum strength in the center. Besides, there are three zero points in the distribution. So we conclude that mixed modes including TM_{01}, TM_{02}, and TM_{03} modes indeed occupy SWS1. The decrease of the E_z near the SWS surface explains why the beam modulation becomes weakened in SWS1 as seen from Figs. 8 and 9.

Table 2. Power proportions of TM_{0n} modes in the middle of the drift tube.

Mode		TM_{01}	TM_{02}	TM_{03}
direction	$+z$	46.8% (6.56 MW)	23.4% (3.28 MW)	29.8% (4.19 MW)
	$-z$	65.7% (14.76 MW)	25.5% (5.74 MW)	8.8% (1.97 MW)

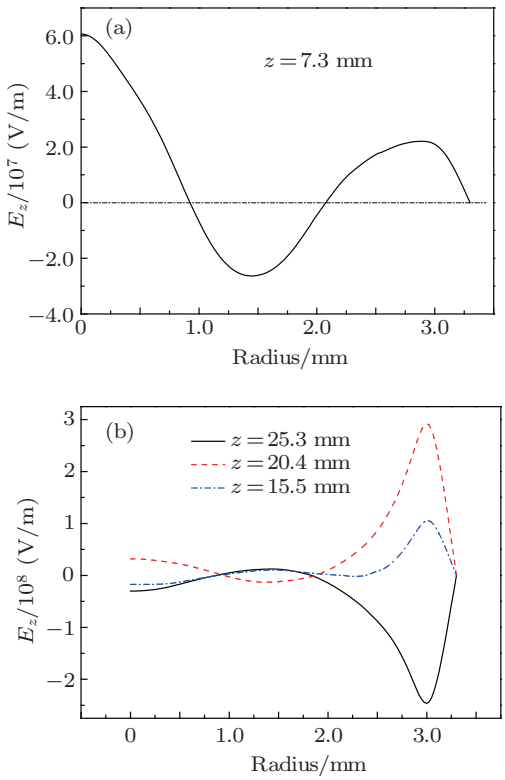


Fig. 11. (color online) Radial distributions of E_z in the two sections of the SWS: (a) SWS1 and (b) SWS2.

Likewise, certain power proportions of TM_{02} and TM_{03} modes would enter into SWS2. However, its Q value is relatively high so that the selection mechanism of TM_{01} mode by electron selection works, and the resonant reciprocal Bragg reflection is achieved all over the whole section. Accordingly, the higher modes come from the inside conversion and the outside import can be suppressed well. Figure 11(b) shows the radial distributions of E_z at three positions of SWS2, and they all accord well with the theoretical distribution of TM_{01} mode surface wave. This implies that the surface wave of

TM_{01} mode is successfully and dominantly excited and amplified in SWS2. So we regard the proposed SWO as a device with single mode operation, yet multi-modes participate in the premodulation of the electron beam.

3.4. Typical simulated performances

For the proposed SWO with the structural parameters listed in Table 1, some typical output performances are simulated by using the UNIPIC code. The radiation spectrum shown in Fig. 12(a) is acquired by the Fourier transform of the time-dependent electric field in SWSs. The central frequency is 146.3 GHz with a $\Delta f/f \approx 1\%$, which is in rough agreement with the synchronism point between the electron beam line and the dispersion curve of TM_{01} mode. This also confirms the proposed SWO as a single mode operation device. Figure 12(b) shows the profile of average output power versus time in the output waveguide, which indicates that the stable output power is about 70MW and the corresponding conversion efficiency is almost 20%, which is the same as the one obtained in Ref. [18] by using an electron beam with an energy of 430 keV and a current of 3.23 kA. Figure 12(b) also demonstrates that the conversion efficiency of the SWO with integral SWS is only 9.3%. Even compared with the efficiency of the previous improved subterahertz overmoded SWOs with integral SWSs and similar beam parameters,[16,17,23] the efficiency of the proposed SWO still increases almost 50%. Besides, as seen from Fig. 12(b), the device reaches the steady state regime of operation at 6 ns after starting with a startup time of about 2.5 ns, while the SWO with integral SWS has a startup time of about 1.9 ns and similar rise time under the normalized amplitude condition. Due to the larger Q value of integral SWS and earlier beam modulation within it, the start-oscillating becomes faster. But the two temporal characteristic parameters of the proposed device are still much smaller than the ones of X band MWCGs and similar devices in millimeter wave frequency band.[10,21] This is beneficial to the miniaturization of the accelerator in practical applications.

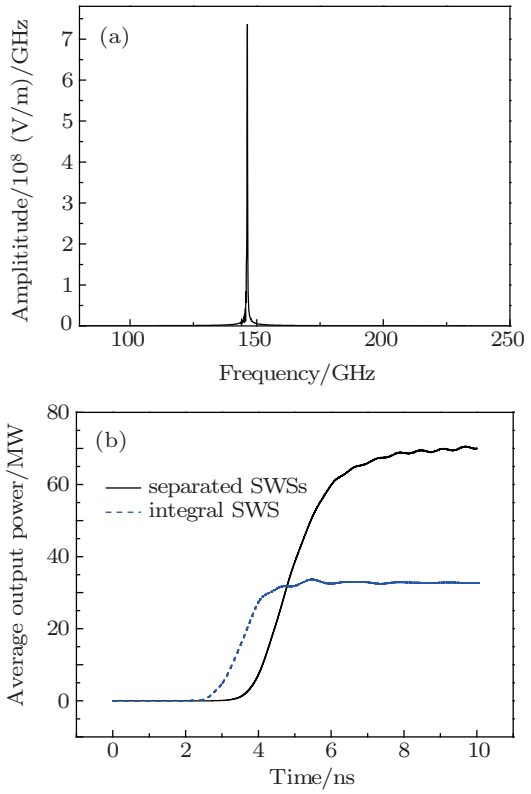


Fig. 12. (color online) Simulated results from the proposed SWO: (a) frequency spectrum and (b) average output power.

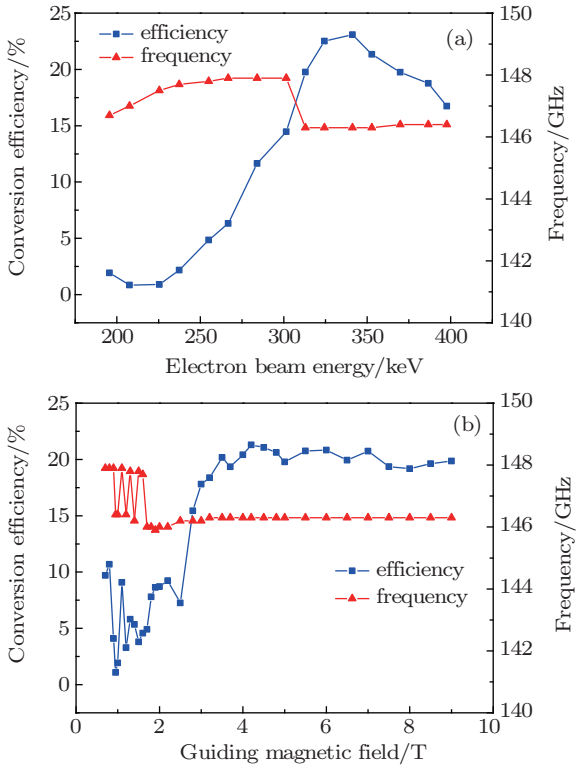


Fig. 13. (color online) Dependences of the conversion efficiency and frequency on (a) beam energy and (b) guiding magnetic field.

The influences of two important adjustable external parameters in actual experiments, i.e., applied diode voltage and guiding magnetic field, on the output performances of the proposed SWO are also simulated. Figure 13 shows the dependences of conversion efficiency and frequency on the electron beam energy (Fig. 13(a)) which is proportional to the applied diode voltage, and on guiding magnetic field (Fig. 13(b)). To ensure that the effective beam-wave interaction occurs in the optimal axial mode, the optimal beam energy ranges from 310 to 370 keV, giving rise to conversion efficiencies around 20% or higher, and the frequency is almost unchanged. When the guiding magnetic field is less than 2 T, the efficiency is sensitive to it while the dominant frequency jumps between about 146.4 GHz and 147.9 GHz. Moreover, there is an obvious efficiency dip near 0.95 T, which agrees well with one of the cyclotron resonance magnetic field strength in Cerenkov devices, i.e., 0.97 T according to the Vlasov's theory.[31] The other one is as high as 19.4 T that exceeds the practical requirement, so

it is not considered in our simulation. The generation efficiencies and frequencies are almost the same in a wide range from 3.5 T to 9 T. Therefore, the guiding magnetic field can be reduced to 3.5 T in the later experiments. Besides, conversion efficiency over 10% is obtained at a guiding magnetic field strength of 0.8 T. So it is believed that the operation of the proposed SWO at low guiding magnetic field is practical and feasible, and higher efficiency by proper structural modification can be expected due to the decreases of both the current density and the space charge effect in overmoded devices.[21]

4. Conclusions

In this work, a subterahertz SWO with separated overmoded SWSs is proposed to achieve high efficiency. The theoretical estimation proves that the proposed device can be driven by electron beam with modest energy and current. This is of advantage to repetitive operation for practical applications. According to the detailed PIC simulation results, there are some important factors to ensure the high efficiency: the premodulation of electron beam and reflection of counter-running wave in the first SWS section, the suppression of beam velocity modulation and enhancement of beam density modulation in the drift tube, and the modest Q value of the second SWS section and fairly pure TM_{01} mode operation within this part. Under the condition of a beam energy of 313 keV, beam current of 1.13 kA, and guiding magnetic field beyond 3.5 T, the proposed SWO can generate a subterahertz wave with a frequency of 146.3 GHz and an output power of 70 MW, yielding an efficiency of about 20%. This high efficiency has been achieved before only by an overmoded 0.14-THz SWO with integral SWS driven by electron beam with much higher energy and current. Moreover, at relatively low magnetic field of 0.8 T, an efficiency exceeding 10% has been obtained from our simulation results. So we believe that higher efficiency will be attained at the magnetic field less than 1 T in the near future by modifying the proposed SWO here.

References

[1] Benford J, Swegle J and Schamiloglu E 2007 *High Power Microwaves*, 2nd edn. (New York: CRC)
[2] Booske J H 2008 *Phys. Plasmas* **15** 055502
[3] Feng W, Zhang R and Cao J C 2013 *Physics* **42** 846 (in Chinese)
[4] Nusinovich G S, Pu R F, Antonsen T M, Sinitsyn O V, Rodgers J, Mohamed A, Silverman J, Sheikhly M A, Dimant Y S and Milikh G M 2011 *J. Infrared Milli. Terahz. Waves* **32** 380
[5] Bratman V L, Denisov G G, Ofitserov M M, Korovin S D, Polevin S D and Rostov V V 1987 *IEEE Trans. Plasma Sci.* **15** 2
[6] Klimov A I, Korovin S D, Rostov V V, Ulmaskulov M R, Shpak V G, Shunailov S A and Yalandin M I 2002 *IEEE Trans. Plasma Sci.* **30** 1120
[7] Zhang K C and Wu Z H 2013 *Acta Phys. Sin.* **62** 024103 (in Chinese)
[8] Zhang K C, Qi Z K and Yang Z L 2015 *Chin. Phys. B* **24** 079402
[9] Min S H, Kwon O J, Sattorov M A, So J K, Park S H, Baek I K, Choi D H, Shin Y M and Park G S 2011 36*th International Conference on Infrared Millimeter and Terahertz Waves* (IRMMW-THz)
[10] Bugaev S P, Cherepenin V A, Kanavets V I, Klimov A I, Kopenkin A D, Koshelev V I, Popov V A and Slepkov A I 1990 *IEEE Trans. Plasma Sci.* **18** 525
[11] Vlasov A N, Shkvarunets A G, Rodgers J C, Carmel Y, Antonsen T M, Abuelfadl T M, Lingze D, Cherepenin V A, Nusinovich G S, Botton M and Granatstein V L 2000 *IEEE Trans. Plasma Sci.* **28** 550
[12] Chen Z, Wang J, Wang Y, Qiao H, Guo W and Zhang D 2014 *Chin. Phys. B* **23** 068402
[13] Wang G Q, Wang J G, Li S, Wang X F, Lu X C and Song Z M 2015 *Acta Phys. Sin.* **64** 050703 (in Chinese)
[14] Ginzburg N S, Zaslavsky V Y, Malkin A M and Sergeev A S 2013 *Technical Phys.* **58** 267
[15] Wang G, Wang J, Tong C, Li X, Wang X, Li S and Lu X 2013 *Phys. Plasmas* **20** 043105
[16] Chen Z, Wang J, Wang G, Li S, Wang Y, Zhang D and Qiao H 2014 *Acta Phys. Sin.* **63** 110703 (in Chinese)
[17] Wang G, Wang J, Li S, Zeng P, Zhang L and Chen Z 2016 *High Power Laser and Particle Beams* **28** 033103 (in Chinese)
[18] Li X, Wang J, Song Z, Chen C, Sun J, Zhang X and Zhang Y 2012 *Phys. Plasmas* **19** 083111
[19] Li X, Wang J, Sun J, Song Z, Ye H, Zhang Y, Zhang L and Zhang L 2013 *IEEE Trans. Electron Dev.* **60** 2931
[20] Grabowski C, Gahl J M and Schamiloglu E 1997 *IEEE Trans. Plasma Sci.* **25** 335
[21] Zhu J, Shu T, Zhang J, Li G and Zhang Z 2010 *Phys. Plasmas* **17** 083104
[22] Wang G, Wang J, Li S and Wang X 2015 *AIP Adv.* **5** 097155
[23] Wang G, Wang J, Zeng P, Li S and Wang D 2016 *Phys. Plasmas* **23** 023104
[24] Minami K, Ogura K, Aiba Y, Amin M R, Zheng X D, Watanabe T, Carmel Y, Destler W W and Granatstein V L 1995 *IEEE Trans. Plasma Sci.* **23** 124
[25] Levush B, Antonsen T M, Bromborsky A, Lou W R and Carmel Y 1992 *IEEE Trans. Plasma Sci.* **20** 263
[26] Wang J, Zhang D, Liu C, Li Y, Wang Y, Wang H, Qiao H and Li X 2009 *Phys. Plasmas* **16** 033108
[27] Wang J, Wang Y and Zhang D 2006 *IEEE Trans. Plasma Sci.* **34** 681
[28] Teng Y, Cao Y, Song Z, Ye H, Shi Y, Chen C and Sun J 2014 *Phys. Plasmas* **21** 123108
[29] Zhang D, Zhang J, Zhong H, Jin Z and Ju J 2014 *Phys. Plasmas* **21** 093102
[30] Wang G, Wang J, Li S, Wang X, Tong C, Lu X and Guo W 2013 *Acta Phys. Sin.* **62** 150701 (in Chinese)
[31] Vlasov A N, Ilyin A S and Carmel Y 1998 *IEEE Trans. Plasma Sci.* **26** 605